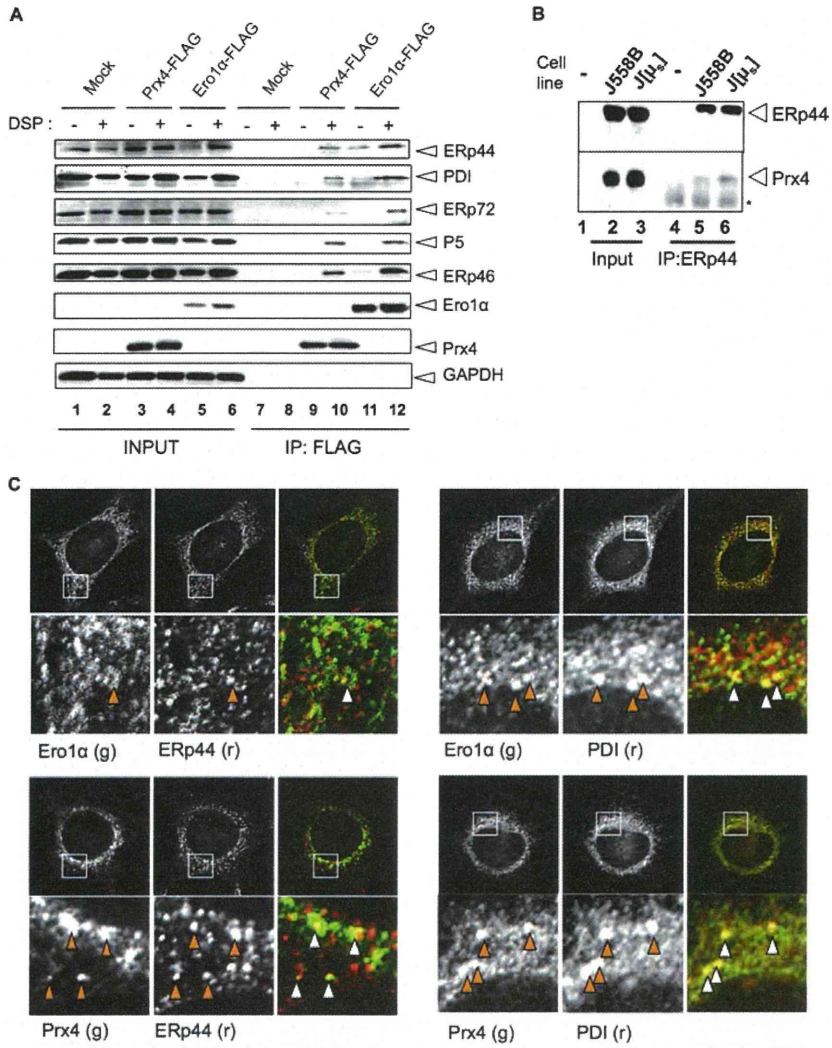

FIGURE 1. **Prx4 and Ero1α share similar partners and subcellular localizations.** *A*, 24 h after transfection with pcDNA3.1, Prx4-FLAG, or Ero1α-FLAG, 10^6 HeLa cells were incubated with or without 0.25 μM dithiobis succinimidyl propionate (*DSP*) on ice. Anti-FLAG immunoprecipitates (*IP*) were then eluted by FLAG peptides and analyzed by Western blot with the indicated antibodies. Aliquots of the total Nonidet P-40 lysates from 10^4 cells (*INPUT*) were loaded to estimate (co)-immunoprecipitation efficiency. *B*, lysates from 10^7 mouse myeloma J558L cells or their derivative expressing nitrophenol-specific secretory Ig-μ chains (*J*[μ_s]) were immunoprecipitated with anti-ERp44 and analyzed by Western blot with the indicated antibodies. The slightly more abundant Prx4 associated to ERp44 in J[μ_s] cells may reflect physiological interactions in the presence of an abundant substrate (7). *C*, HeLa cells were fixed by 4% paraformaldehyde and permeabilized by 0.2% Triton X-100. Co-localization of Prx4 or Ero1α with PDI or ERp44 was observed by immunofluorescence using the indicated fluorochrome-conjugated antibodies, as described under "Experimental Procedures." *g*, green. *r*, red.

lyzed their binding properties *in vitro* by surface plasmon resonance (SPR) assays and estimated the k_{on}, k_{off}, and K_D values. PDI bound Ero1α with ~5.5-fold stronger affinity than Prx4 at pH 7.4, which is similar to the pH in the ER (1.94 and 10.6 μM, respectively, Fig. 3*A* and supplemental Fig. 3). In contrast, the two enzymes displayed similar affinities for ERp44 at pH 6.4 (5.15 and 6.92 μM, for Ero1α and Prx4, respectively). The affinity of ERp44 to Ero1α and Prx4 was decreased at pH 7.4 in comparison with that at pH 6.4 (Fig. 3*A* and supplemental Fig. 3), suggesting that ERp44 binds Prx4 more effectively at low pH like in the distal ESC stations (10.4 and 17.9 μM for Ero1α and Prx4, respectively) (12). Extrapolating these *in vitro* results to the cellular environment, PDI would preferentially retain Ero1α in the ER.

To challenge this possibility, we co-expressed increasing amounts of PDI-FLAG with constant levels of Ero1α-FLAG and Prx4-FLAG in HeLa cells. 24 h after transfection, culture media and cell lysates were analyzed by Western blot (Fig. 3*B*) and quantified (Fig. 3*D*). Consistent with the *in vitro* results shown in Fig. 3*A*, Ero1α secretion was primarily inhibited by PDI, whereas higher levels of expression of PDI were required to retain Prx4 (Fig. 3, *B* and *D*). In contrast, HA-ERp44 inhibited secretion of Ero1α-FLAG and Prx4-FLAG to similar extents. Collectively, these results indicate that PDI binds and retains Ero1α more efficiently than Prx4.

Sequential Interactions of Ero1α and Prx4 with PDI and ERp44 in ESC—In view of their different distributions along ESC (7, 8), PDI and ERp44 might exert sequential effects on the

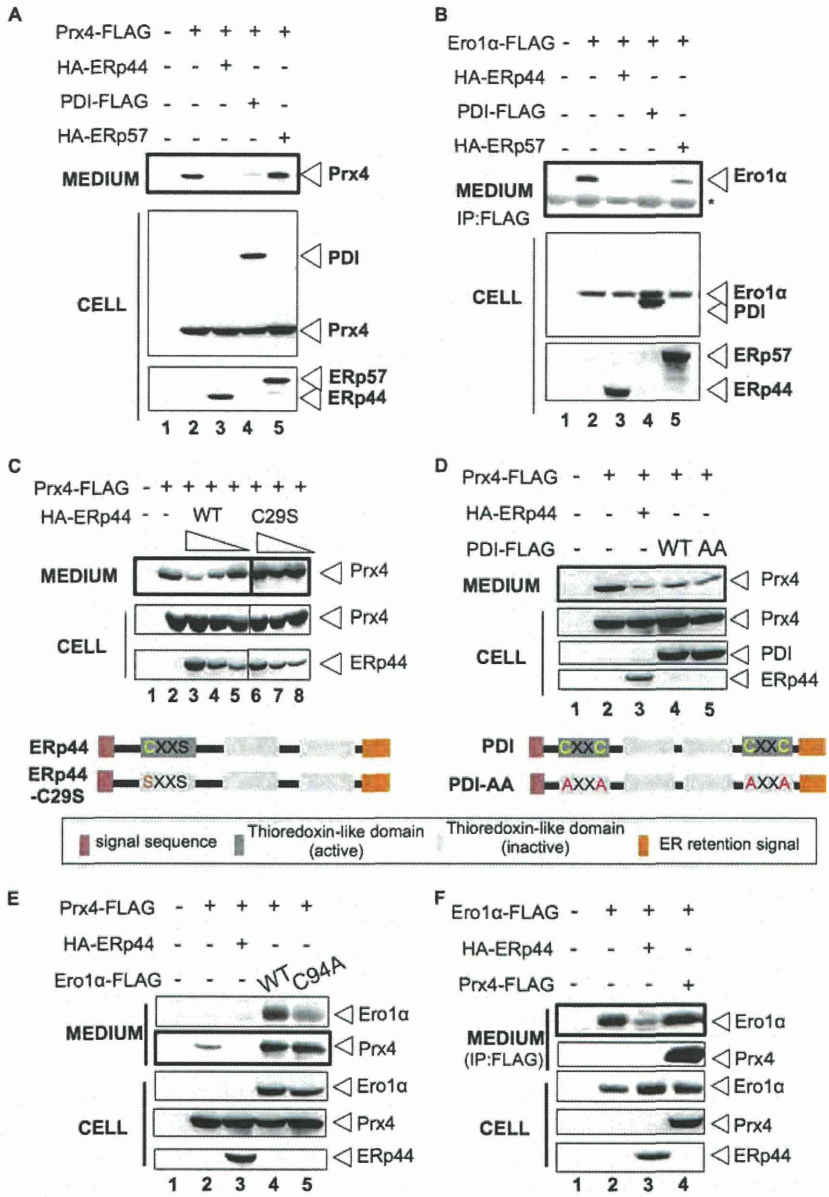

FIGURE 2. **Dynamic retention of Prx4 by ERp44 and PDI.** *A* and *B*, HeLa cells were co-transfected with Prx4-FLAG (*A*) or Ero1α-FLAG (*B*) and HA-ERp44, PDI-FLAG, or HA-ERp57 as indicated. 24 h after transfection, cells were cultured in FBS-free Opti-MEM medium for 5 h. The spent medium was subsequently precipitated with 15% TCA (*A*) or anti-FLAG antibodies (*B*) and analyzed by Western blot with the indicated antibodies. *C*, Prx4-FLAG was co-expressed in HeLa cells with increasing amounts of HA-ERp44-WT or the C29S mutant (9). 24 h after transfection, cells were handled as described for *panels A* and *B*. When compared with cells overexpressing Prx4-FLAG alone (*lane 2*), Prx4 secretion was inhibited by high levels of ERp44-WT (*lanes 3–5*) but not by ERp44-C29S (*lanes 6–8*). *D*, wild type (PDI-WT-FLAG) or a mutant PDI (PDI-AA-FLAG) in which all four cysteines in the a- and a′-domains had been mutated to alanine were co-expressed with Prx4-FLAG in HeLa cells and handled as above. When compared with cells overexpressing Prx4-FLAG alone (*lane 2*), both PDI-WT and the AA mutant retained Prx4 (*lanes 4* and *5*). *E* and *F*, wild type (Ero1α-FLAG) or an enzymatically inactive variant (Ero1α-C94A-FLAG) was co-expressed with Prx4 in HeLa cells. Clearly, Prx4 secretion was dramatically increased by co-expression of either Ero1α-FLAG or Ero1α-C94A-FLAG. In the experiment shown in *panel F*, Prx4-FLAG was co-expressed with Ero1α-FLAG in HeLa cells. Unlike what observed in *panel E*, retention of Ero1α was not competed by Prx4-FLAG co-expression.

localization/retention of Ero1α and Prx4. Therefore, we compared the effects of silencing ERp44, PDI, or both on the secretion of endogenous Prx4 and Ero1α by HeLa cells (Fig. 4*A*). Individual siRNAs for ERp44 or PDI effectively silenced the respective targets (Fig. 4*A*, *lanes 7–12*, *right panel*). Lowering the levels of ERp44 greatly promoted secretion of endogenous Prx4 (Fig. 4*A*, *lanes 1–3*, *upper*), but only marginally affected Ero1α retention (Fig. 4*A*, *lanes 1–3*, *lower*, and Fig. 4*C*, *upper*). Thus, under physiological conditions, PDI seems to retain Ero1α sufficiently. Neither endogenous Prx4 nor Ero1α was released by lowering the levels of PDI alone in HeLa cells (Fig. 4*A*, *lanes 4* and *5*, and Fig. 4*C*, *middle*). Considering that ERp44 is localized downstream with respect to PDI in the ESC, we surmised that ERp44 acted as a backup retention machinery in

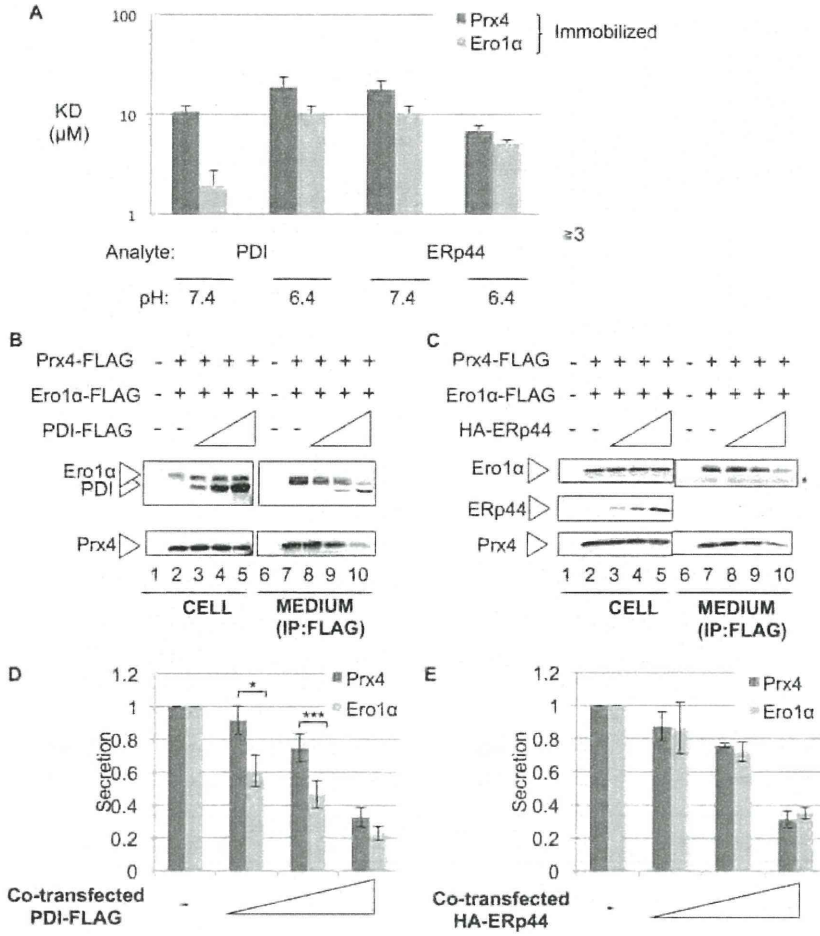

FIGURE 3. **Ero1α competes with Prx4 for PDI but not for ERp44 binding.** *A*, purified human Ero1α or Prx4 proteins were immobilized on a biosensor chip, and PDI or ERp44 was injected as analyte. The affinity of PDI for Ero1α is about 5.5-fold stronger than Prx4, whereas ERp44 interacts similarly with Ero1α or Prx4. *B–E*, Prx4-FLAG and Ero1α-FLAG were co-expressed with increasing amounts of PDI-FLAG (*B* and *D*) or HA-ERp44 (*C* and *E*) in HeLa cells. 24 h after transfection, cells were cultured in Opti-MEM for 4 h. Aliquots from cell lysates or anti-FLAG immunoprecipitates (*IP*) from the spent medium were analyzed by Western blotting (*D* and *E*) and quantified by densitometry. $n = 3$. *, $p < 0.05$, ***, $p < 0.001$.

the absence of PDI (Fig. 4*C*, *middle*). Accordingly, the simultaneous silencing of ERp44 and PDI allowed secretion of both endogenous Ero1α and endogenous Prx4 by HeLa cells (Fig. 4*A*, *lane 6*). Backup mechanism by ERp44 was further confirmed by immunofluorescence of HeLa cells transfected with nonspecific siRNA or specific PDI. Endogenous PDI was efficiently silenced by RNAi (supplemental Fig. 4). As expected, co-localization of ERp44 with Ero1α and Prx4 was increased in PDI-silenced cells (Fig. 5*B*), whereas such a condition did not affect the morphology of the ER or ERGIC (supplemental Fig. 4), suggesting that retention of Ero1α and Prx4 in ESC depends mostly on ERp44 in the absence of PDI. Thus, sequential interactions with PDI and ERp44 underlie the intracellular retention of Prx4 and Ero1α. Ero1α displays higher affinity for PDI, but in its absence, it can be retrieved by ERp44. On the other hand, Prx4 is mainly retained by ERp44 because of its lower affinity for PDI (Fig. 3*A*).

Lack of ER Retention Signals in Two ER Oxidases Is Important for ER Redox Homeostasis—In virtually all vertebrates, Ero1α and Prx4 do not harbor ER retention signals (25) (supplemental Fig. 1). As Ero1α and Prx4 play major roles in oxidative protein folding, we surmised that the stepwise retention/localization mechanism of these two ER oxidases in higher eukaryotes may be important for ER redox regulation. To monitor ER redox balance, therefore, we exploited ERroGFPiE. This sensor co-localized with ER-targeted DsRed2 (supplemental Fig. 5). As shown by Birk *et al.* (31), ERroGFPiE can be resolved into two bands under nonreducing conditions corresponding to its reduced (*i.e.* DTT-treated) and oxidized (*i.e.* dipyridyl disulfide-treated) isoforms (Fig. 5*A*, *lanes 2–4*). As indicated by the accumulation of reduced ERroGFPiE and consistent with the notion that Ero1α is a prominent ER oxidase, its knockdown caused hypo-oxidizing condition in the ER (Fig. 5*A*, *lane 7*). Next, we monitored the ER redox state in cells expressing KDEL-extended or wild type Ero1α. Surprisingly, expression of Ero1α-KDEL caused a more oxidizing shift in ERroGFPiE than wild type Ero1α (Fig. 5*A*, *lanes 5* and *6*). Similar results were obtained appending a KDEL motif to Prx4 (Fig. 5*B*). The co-expression of Ero1α with Prx4-KDEL caused a much more dramatic oxidative shift to the redox balance in the ER (Fig. 5*B*, *lane 6*). Taken together, our results strongly suggest that the

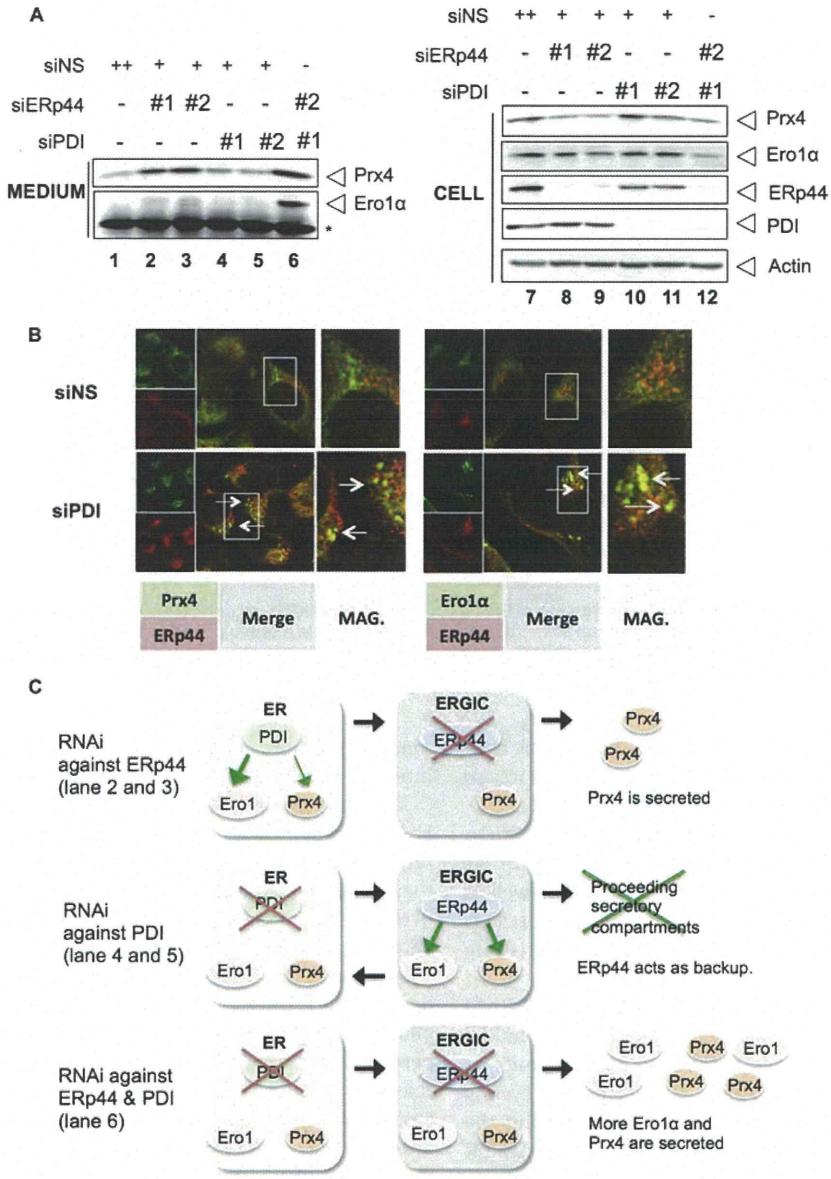

FIGURE 4. **Silencing ERp44 allows secretion of endogenous Prx4, but not Ero1α.** *A*, secretion of endogenous Prx4 or Ero1α by HeLa cells was analyzed with RNAi for nonspecific (*NS*) ERp44 or PDI (*lanes 1–5*) or both (*lane 6*) by specific siRNAs. 72 h after transfection, cells were cultured in Opti-MEM for 6 h and analyzed as described in the legend for Fig. 2. *B*, immunofluorescence of HeLa cells transfected with nonspecific siRNA (*siNS*) or PDI siRNA (*siPDI*). Endogenous Prx4 or Ero1α was co-stained with endogenous ERp44. In PDI-silenced cells the co-localization of Prx4 or Ero1α with ERp44 was more intense, consistent with a backup role of ERp44. *siERp44*, ERp44 siRNA. *C*, strategy utilized to dissect the retention of Ero1α and Prx4.

dynamic, stepwise retention mechanisms of Ero1α and Prx4 are important for fine-tuning the redox status along the ESC.

DISCUSSION

Our studies have established that two ER oxidases, Ero1α and Prx4, share a noncanonical retention mechanism in the ER. Knockdown of PDI exerted little effect on the secretion of Ero1α and Prx4, whereas knockdown of ERp44 allowed secretion of endogenous Prx4. This observation suggests that Prx4 retention is controlled mainly by ERp44 under physiological conditions. On the other hand, knockdown of both ERp44 and PDI caused marked secretion of Ero1α and Prx4. The different affinity of PDI for Ero1α and Prx4 partially explains why the former was mainly retained by PDI in the ER. After PDI knockdown, the localization of both Ero1α and Prx4 was changed from an ER pattern to a more vesicular pattern containing ERp44. Taken together, these observations strongly suggest that Ero1α and Prx4 are mainly retained by PDI in the proximal ESC. Because of its lower affinity for PDI, some Prx4 continuously reaches the distal ESC stations, from which it is retrieved by ERp44 in a pH-dependent manner, as described for overexpressed Ero1α or IgM subunits (12). In this scenario, ERp44

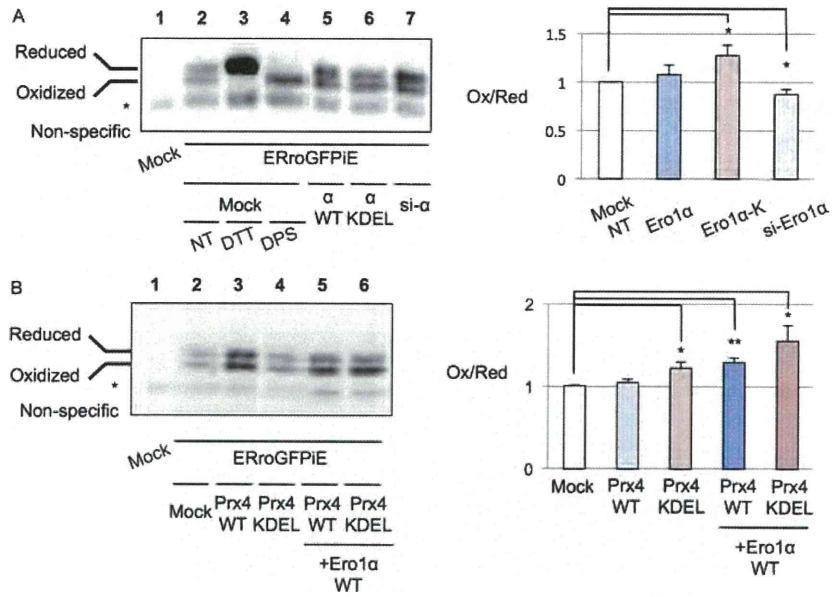

FIGURE 5. **Increased oxidation of ERroGFPiE upon co-expression of Ero1αKDEL and/or Prx4KDEL.** *A* and *B*, ERroGFPiE is transiently overexpressed in HeLa cells. Reductive or oxidative shift in the ER redox of cells indicated was detected in nonreducing Western blot and quantified. The average ratios of intensity of the oxidized band to the reduced band are depicted in graphs, which are standardized by the ratio of samples of nontreated (*NT*) cells (*lane 2*). $n = 3$. *, $p < 0.05$, **, $p < 0.01$. *DPS*, dipyridyl disulfide; *si-α*, Ero1α siRNA; *si-Ero1α*, Ero1α siRNA; *Ox/Red*, oxidized/reduced.

acts as a backup system. This multistep retention seems conserved throughout evolution; indeed, almost all vertebrates so far reported lack KDEL-like motifs (supplemental Fig. 1).

It is noteworthy that appending KDEL-like motifs to Ero1α or Prx4 caused hyperoxidizing conditions in the ER (Fig. 5). As suitable redox homeostasis is required for efficient as well as accurate oxidative protein folding in the ER (26), our results argue in favor of a physiological role for the dynamic retention of the two ESC oxidases.

An important result emerging from our studies is that ERp44 binds Prx4 more strongly at acidic pH. ERp44 is a unique PDI family member whose conserved CRFS active motif limits its potential function as an oxidoreductase. As a chaperone cycling in ESC, ERp44 preferentially binds its client proteins in the acidic environment of cis Golgi to retrieve them into the ER (12). Its lower affinity at neutral pH likely favors client release in the ER.

Because of their similar interaction patterns, Ero1α and Prx4 largely co-localize; their vicinity may optimize productive folding while limiting H_2O_2 production and oxidative stress. However, H_2O_2 is not only a foe, but can be utilized as an intra- or intercellular signaling device (32, 33). Therefore, it will be of interest to determine whether the relative levels of Ero1α, Prx4, and their retainer molecules differ between cell types or differentiation states. Besides its key potential role in maintaining redox homeostasis, the dynamic retention mechanism of Ero1α and Prx4 appears to generate a gradient of the two oxidases within the ESC. Considering its possible regulation by pH, such a gradient might have relevant functional consequences. Ero1α has been detected on platelet surface in association with PDI, where it might regulate integrin function (34). Particularly in cells establishing close contacts (*i.e.* immunological or neural synapses), export of redox-active molecules might regulate the intensity and duration of intercellular cross-talks.

The thiol group (-SH) of peroxidatic cysteine is oxidized by H_2O_2 to sulfenic acid (-SOH). At higher concentrations, H_2O_2 further oxidizes the sulfenic moieties to sulfinic ($-SO_2H$) and then sulfonic acid ($-SO_3H$). Prx4 can undergo hyperoxidation in the ER lumen (35); however, no sulfiredoxin activity has been detected so far in the secretory compartment. Therefore, sulfinylated or sulfonylated Prx4 is likely degraded or released, perhaps acting as intercellular signals. Prx4 is retained by thiol-dependent mechanisms (Fig. 1*C*), and modifications of the peroxidatic cysteines might lead to secretion. However, Prx4 release was similar in cells overexpressing wild type Ero1α or an enzymatically inactive mutant (Fig. 2*E*), suggesting that Ero1α does not weaken Prx4 retention via H_2O_2 production, but likely via competitive binding. However, additional H_2O_2 sources may cause Prx4 hyperoxidation and release (15). It should be important and interesting to examine whether and how the interactive retention mode of Ero1α and Prx4 regulates oxidative folding of nascent proteins and whether and how it can adapt to changing physiological requirements.

Acknowledgment—We thank Dr. Neil J. Bulleid for the generous gift of construct of ERroGFPiL.

REFERENCES

1. Hatahet, F., and Ruddock, L. W. (2009) Protein disulfide isomerase: a critical evaluation of its function in disulfide bond formation. *Antioxid. Redox Signal.* **11,** 2807–2850
2. Inaba, K., Masui, S., Iida, H., Vavassori, S., Sitia, R., and Suzuki, M. (2010) Crystal structures of human Ero1α reveal the mechanisms of regulated and targeted oxidation of PDI. *EMBO J.* **29,** 3330–3343

3. Masui, S., Vavassori, S., Fagioli, C., Sitia, R., and Inaba, K. (2011) Molecular bases of cyclic and specific disulfide interchange between human ERO1α protein and protein-disulfide isomerase (PDI). *J. Biol. Chem.* **286,** 16261–16271
4. Wang, L., Wang, L., Vavassori, S., Li, S., Ke, H., Anelli, T., Degano, M., Ronzoni, R., Sitia, R., Sun, F., and Wang, C. C. (2008) Crystal structure of human ERp44 shows a dynamic functional modulation by its carboxy-terminal tail. *EMBO Rep.* **9,** 642–647
5. Cortini, M., and Sitia, R. (2010) From antibodies to adiponectin: role of ERp44 in sizing and timing protein secretion. *Diabetes Obes. Metab.* **12,** Suppl. 2, 39–47
6. Gilchrist, A., Au, C. E., Hiding, J., Bell, A. W., Fernandez-Rodriguez, J., Lesimple, S., Nagaya, H., Roy, L., Gosline, S. J., Hallett, M., Paiement, J., Kearney, R. E., Nilsson, T., and Bergeron, J. J. (2006) Quantitative proteomics analysis of the secretory pathway. *Cell* **127,** 1265–1281
7. Anelli, T., Ceppi, S., Bergamelli, L., Cortini, M., Masciarelli, S., Valetti, C., and Sitia, R. (2007) Sequential steps and checkpoints in the early exocytic compartment during secretory IgM biogenesis. *EMBO J.* **26,** 4177–4188
8. Fraldi, A., Zito, E., Annunziata, F., Lombardi, A., Cozzolino, M., Monti, M., Spampanato, C., Ballabio, A., Pucci, P., Sitia, R., and Cosma, M. P. (2008) Multistep, sequential control of the trafficking and function of the multiple sulfatase deficiency gene product, SUMF1 by PDI, ERGIC-53 and ERp44. *Hum. Mol. Genet.* **17,** 2610–2621
9. Anelli, T., Alessio, M., Bachi, A., Bergamelli, L., Bertoli, G., Camerini, S., Mezghrani, A., Ruffato, E., Simmen, T., and Sitia, R. (2003) Thiol-mediated protein retention in the endoplasmic reticulum: the role of ERp44. *EMBO J.* **22,** 5015–5022
10. Wang, Z. V., Schraw, T. D., Kim, J. Y., Khan, T., Rajala, M. W., Follenzi, A., and Scherer, P. E. (2007) Secretion of the adipocyte-specific secretory protein adiponectin critically depends on thiol-mediated protein retention. *Mol. Cell. Biol.* **27,** 3716–3731
11. Araki, K., and Inaba, K. (2012) Structure, mechanism, and evolution of Ero1 family enzymes. *Antioxid. Redox Signal.* **16,** 790–799
12. Vavassori, S., Cortini, M., Masui, S., Sannino, S., Anelli, T., Caserta, I. R., Fagioli, C., Mossuto, M. F., Fornili, A., van Anken, E., Degano, M., Inaba, K., and Sitia, R. (2013) A pH-regulated quality control cycle for surveillance of secretory protein assembly. *Mol. Cell* **50,** 783–792
13. Zito, E., Melo, E. P., Yang, Y., Wahlander, Å., Neubert, T. A., and Ron, D. (2010) Oxidative protein folding by an endoplasmic reticulum-localized peroxiredoxin. *Mol. Cell* **40,** 787–797
14. Tavender, T. J., Springate, J. J., and Bulleid, N. J. (2010) Recycling of peroxiredoxin IV provides a novel pathway for disulphide formation in the endoplasmic reticulum. *EMBO J.* **29,** 4185–4197
15. Zito, E., Hansen, H. G., Yeo, G. S., Fujii, J., and Ron, D. (2012) Endoplasmic reticulum thiol oxidase deficiency leads to ascorbic acid depletion and noncanonical scurvy in mice. *Mol. Cell* **48,** 39–51
16. Mezghrani, A., Fassio, A., Benham, A., Simmen, T., Braakman, I., and Sitia, R. (2001) Manipulation of oxidative protein folding and PDI redox state in mammalian cells. *EMBO J.* **20,** 6288–6296
17. Araki, K., Iemura, S., Kamiya, Y., Ron, D., Kato, K., Natsume, T., and Nagata, K. (2013) *J. Cell Biol.* **202,** 861–874
18. Jessop, C. E., Watkins, R. H., Simmons, J. J., Tasab, M., and Bulleid, N. J. (2009) Protein disulphide isomerase family members show distinct substrate specificity: P5 is targeted to BiP client proteins. *J. Cell Sci.* **122,** 4287–4295
19. Appenzeller-Herzog, C., Riemer, J., Zito, E., Chin, K. T., Ron, D., Spiess, M., and Ellgaard, L. (2010) Disulphide production by Ero1α-PDI relay is rapid and effectively regulated. *EMBO J.* **29,** 3318–3329
20. Otsu, M., Bertoli, G., Fagioli, C., Guerini-Rocco, E., Nerini-Molteni, S., Ruffato, E., and Sitia, R. (2006) Dynamic retention of Ero1α and Ero1β in the endoplasmic reticulum by interactions with PDI and ERp44. *Antioxid. Redox Signal.* **8,** 274–282
21. Kakihana, T., Nagata, K., and Sitia, R. (2012) Peroxides and peroxidases in the endoplasmic reticulum: integrating redox homeostasis and oxidative folding. *Antioxid. Redox Signal.* **16,** 763–771
22. Ronzoni, R., Anelli, T., Brunati, M., Cortini, M., Fagioli, C., and Sitia, R. (2010) Pathogenesis of ER storage disorders: modulating Russell body biogenesis by altering proximal and distal quality control. *Traffic* **11,** 947–957
23. Natsume, T., Yamauchi, Y., Nakayama, H., Shinkawa, T., Yanagida, M., Takahashi, N., and Isobe, T. (2002) A direct nanoflow liquid chromatography-tandem mass spectrometry system for interaction proteomics. *Anal. Chem.* **74,** 4725–4733
24. Araki, K., and Nagata, K. (2011) Functional *in vitro* analysis of the ERO1 protein and protein-disulfide isomerase pathway. *J. Biol. Chem.* **286,** 32705–32712
25. Kanehisa, M., and Goto, S. (2000) KEGG: Kyoto Encyclopedia of Genes and Genomes. *Nucleic Acids Res.* **28,** 27–30
26. Zito, E. (2013) PRDX4, an endoplasmic reticulum-localized peroxiredoxin at the crossroads between enzymatic oxidative protein folding and nonenzymatic protein oxidation. *Antioxid. Redox Signal.* **18,** 1666–1674
27. Fagioli, C., Mezghrani, A., and Sitia, R. (2001) Reduction of interchain disulfide bonds precedes the dislocation of Ig-μ chains from the endoplasmic reticulum to the cytosol for proteasomal degradation. *J. Biol. Chem.* **276,** 40962–40967
28. Anelli, T., Bergamelli, L., Margittai, E., Rimessi, A., Fagioli, C., Malgaroli, A., Pinton, P., Ripamonti, M., Rizzuto, R., and Sitia, R. (2012) Ero1α regulates Ca^{2+} fluxes at the endoplasmic reticulum-mitochondria interface (MAM). *Antioxid. Redox Signal.* **16,** 1077–1087
29. Gilady, S. Y., Bui, M., Lynes, E. M., Benson, M. D., Watts, R., Vance, J. E., and Simmen, T. (2010) Ero1α requires oxidizing and normoxic conditions to localize to the mitochondria-associated membrane (MAM). *Cell Stress Chaperones* **15,** 619–629
30. Okado-Matsumoto, A., Matsumoto, A., Fujii, J., and Taniguchi, N. (2000) Peroxiredoxin IV is a secretable protein with heparin-binding properties under reduced conditions. *J. Biochem.* **127,** 493–501
31. Birk, J., Meyer, M., Aller, I., Hansen, H. G., Odermatt, A., Dick, T. P., Meyer, A. J., and Appenzeller-Herzog, C. (2013) Endoplasmic reticulum: reduced and oxidized glutathione revisited. *J. Cell Sci.* **126,** 1604–1617
32. Bae, Y. S., Oh, H., Rhee, S. G., and Yoo, Y. D. (2011) Regulation of reactive oxygen species generation in cell signaling. *Mol. Cells* **32,** 491–509
33. Niethammer, P., Grabher, C., Look, A. T., and Mitchison, T. J. (2009) A tissue-scale gradient of hydrogen peroxide mediates rapid wound detection in zebrafish. *Nature* **459,** 996–999
34. Swiatkowska, M., Padula, G., Michalec, L., Stasiak, M., Skurzynski, S., and Cierniewski, C. S. (2010) Ero1α is expressed on blood platelets in association with protein-disulfide isomerase and contributes to redox-controlled remodeling of αIIbβ3. *J. Biol. Chem.* **285,** 29874–29883
35. Tavender, T. J., and Bulleid, N. J. (2010) Peroxiredoxin IV protects cells from oxidative stress by removing H_2O_2 produced during disulphide formation. *J. Cell Sci.* **123,** 2672–2679

MCB
Journals.ASM.org

The Casein Kinase 2-Nrf1 Axis Controls the Clearance of Ubiquitinated Proteins by Regulating Proteasome Gene Expression

Yoshiki Tsuchiya,[a] Hiroaki Taniguchi,[a] Yoshiyuki Ito,[a] Tomoko Morita,[a] M. Rezaul Karim,[a] Norihito Ohtake,[a] Kousuke Fukagai,[a] Takao Ito,[a] Shota Okamuro,[a] Shun-ichiro Iemura,[b] Tohru Natsume,[b] Eisuke Nishida,[c] Akira Kobayashi[a]

Laboratory for Genetic Code, Graduate School of Life and Medical Sciences, Doshisha University, Kyotanabe, Japan[a]; National Institutes of Advanced Industrial Science and Technology, Biological Information Research Center (JBIRC), Kohtoh-ku, Tokyo, Japan[b]; Department of Cell and Developmental Biology, Graduate School of Biostudies, Kyoto University, Kyoto, Japan[c]

Impairment of the ubiquitin-proteasome system (UPS) has been implicated in the pathogenesis of human diseases, including neurodegenerative disorders. Thus, stimulating proteasome activity is a promising strategy to ameliorate these age-related diseases. Here we show that the protein kinase casein kinase 2 (CK2) regulates the transcriptional activity of Nrf1 to control the expression of the proteasome genes and thus the clearance of ubiquitinated proteins. We identify CK2 as an Nrf1-binding protein and find that the knockdown of CK2 enhances the Nrf1-dependent expression of the proteasome subunit genes. Real-time monitoring of proteasome activity reveals that CK2 knockdown alleviates the accumulation of ubiquitinated proteins upon proteasome inhibition. Furthermore, we identify Ser 497 of Nrf1 as the CK2 phosphorylation site and demonstrate that its alanine substitution (S497A) augments the transcriptional activity of Nrf1 and mitigates proteasome dysfunction and the formation of p62-positive juxtanuclear inclusion bodies upon proteasome inhibition. These results indicate that the CK2-mediated phosphorylation of Nrf1 suppresses the proteasome gene expression and activity and thus suggest that the CK2-Nrf1 axis is a potential therapeutic target for diseases associated with UPS impairment.

Accumulation of misfolded and ubiquitinated proteins is a common pathological feature of various human diseases, such as amyotrophic lateral sclerosis (ALS), inclusion body myopathies, alcoholic and nonalcoholic steatohepatitis, and neurodegenerative disorders, including Alzheimer's, Parkinson's, and Huntington's disease (1–3). Multiple lines of evidence suggest that both the ubiquitin-proteasome system (UPS) and autophagy are responsible for the clearance of ubiquitinated proteins that would accumulate in these age-related diseases. It has been demonstrated that the 26S proteasome can degrade soluble ubiquitinated proteins but not the insoluble aggregates, which are targeted by the autophagy-lysosome pathway (4–7). Impairment of proteasome activity is known to cause proteins that are normally turned over by the UPS to aggregate and form inclusion bodies. Thus, it is expected that the upregulation of proteasome activity could prevent inclusion body formation and mitigate the progression of neurodegenerative and related diseases that are caused by the accumulation of abnormal proteins.

Nrf1 (nuclear factor E2-related factor 1 or Nfe2l1) is a member of the Cap'n'Collar (CNC) family of basic leucine zipper (bZip) transcription factors, which also includes p45 NF-E2, Nrf2, and Nrf3 (8, 9). Nrf1 regulates its target gene expression through either the antioxidant response element (ARE) or the Maf recognition element (MARE) by heterodimerizing with small Maf proteins (8, 9). Several gene targeting studies have implicated Nrf1 in the regulation of cellular homeostasis in embryos, hepatocytes, and osteoclasts (10–14). Recent studies have revealed that Nrf1 also plays an essential role in maintaining neuronal cells and that the loss of Nrf1 induces neurodegeneration and abnormal accumulation of ubiquitinated protein aggregates in neurons (15, 16). The impairment of protein homeostasis that is induced by Nrf1 deficiency may be due to the decreased expression of proteasome subunits in these neurons (16). Indeed, Nrf1 controls the expression of proteasome subunit genes in mammalian cells under proteasome dysfunction (17, 18). Therefore, it is critically important to reveal the role of Nrf1 in the regulation of proteasome gene expression and to elucidate the molecular mechanisms underlying the regulation of Nrf1 activity.

In this study, we reveal that the vast majority of proteasome subunit genes and some proteasome-associated genes are under the transcriptional control of Nrf1. We identify the protein kinase casein kinase 2 (CK2) as an Nrf1-interacting protein and demonstrate that CK2 controls proteasome gene expression and activity by suppressing the transcriptional activity of Nrf1. A mutation of the CK2 phosphorylation site of Nrf1 enhances the proteasome activity and reduces the formation of juxtanuclear inclusion bodies. Thus, our work proposes that the CK2-Nrf1 axis could be a new regulatory target for the efficient clearance of ubiquitinated proteins.

MATERIALS AND METHODS

Antibodies. The antibodies utilized in this study were normal rabbit IgG (Santa Cruz), anti-Flag (M2; Sigma), anti-α-tubulin (DM1A; Sigma), antihemagglutinin (anti-HA) (Y-11; Santa Cruz), anti-green fluorescent protein (anti-GFP) (B-2; Santa Cruz), anti-Nrf1 (H-285; Santa Cruz), anti-MafK (C-16; Santa Cruz), anti-CK2α (1AD9; Santa Cruz), anti-CK2α′ (ab10474; Abcam), anti-CK2β (6D5; Santa Cruz), anti-p62/

Received 15 September 2012 Returned for modification 10 October 2012
Accepted 6 June 2013
Published ahead of print 1 July 2013
Address correspondence to Akira Kobayashi, akobayas@mail.doshisha.ac.jp.
M.R.K., N.O., K.F., T.I., and S.O. contributed equally to this work.
Supplemental material for this article may be found at http://dx.doi.org/10.1128/MCB.01271-12.

doi:10.1128/MCB.01271-12

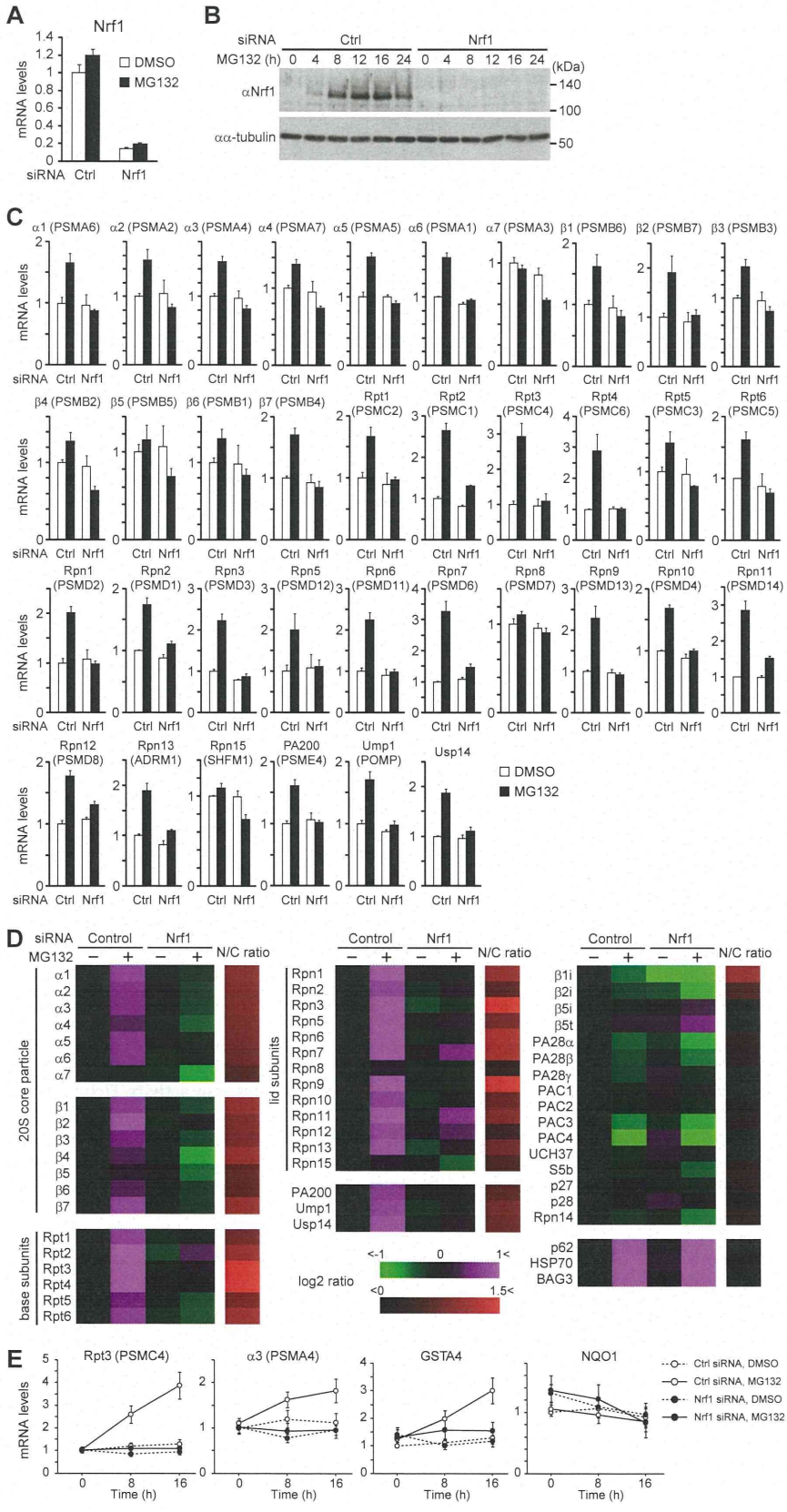

SQSTM1 (PM045; MBL), antiubiquitin (P4D1; Santa Cruz), and anti-LC3 (PD014; MBL). The rabbit polyclonal antibodies directed against mouse Nrf1 that were used in chromatin immunoprecipitation (ChIP) experiments were raised by immunizing rabbits with a purified recombinant six-histidine (6×His)-tagged Nrf1 protein (residues 292 to 741) that was expressed in *Escherichia coli*. The resultant antibodies were subjected to affinity purification.

Plasmids and recombinant proteins. The 3×Flag mouse Nrf1 expression plasmid was described previously (19). Human CK2α (hCK2α) and hCK2β cDNAs were subcloned into pcDNA3 (HA). The ubiquitin-fused luciferase reporter (Ub-FL) reporter plasmid was kindly provided by David Piwnica-Worms (20). The 3xPSMA4-ARE-Luc (Luc stands for luciferase) plasmid was kindly provided by Raymond J. Deshaies (17). The pRBGP2-Luciferase plasmid was described previously (21). The MafK expression plasmid was described previously (22). PCR-amplified Nrf1 fragments were subcloned into pET-15b. Recombinant 6× histidine-tagged Nrf1 fragments were expressed in *E. coli* and purified with nickel-nitrilotriacetic acid (Ni-NTA)–agarose (Qiagen). Recombinant CK2α was described previously (23).

Cell culture and transfection. HeLa cells, COS7 cells, and MCF10A cells were cultured in Dulbecco's modified Eagle's medium (DMEM) (Wako) that was supplemented with 10% fetal calf serum (FCS) (Invitrogen), 4,500 mg/liter glucose, 40 μg/ml streptomycin, and 40 units/ml penicillin. Mouse embryonic fibroblasts (MEFs) were cultured in Iscove's modified Dulbecco's medium (IMDM) (Wako) that was supplemented with 10% FCS, 2 mM glutamine (Invitrogen), 40 μg/ml streptomycin, and 40 units/ml penicillin. The transfection of plasmid DNA and small interfering RNA (siRNA) was achieved using Lipofectamine Plus and Lipofectamine 2000 (Invitrogen), respectively.

siRNA knockdown experiment. The cells were cultured for 24 h in medium without antibiotics. The cells were transfected twice with 40 nM siRNA (at 24 and 48 h after plating) using Lipofectamine 2000. The sequences of the siRNAs employed in the present study are listed in Table S3 in the supplemental material. Twenty-four hours after the last transfection, the cells were utilized for each experiment. For immunoblot analysis, the cells were lysed with an SDS sample buffer (50 mM Tris-HCl [pH 6.8], 10% glycerol, and 1% SDS), and the resultant whole-cell extracts were subjected to immunoblotting with the antibodies indicated in Fig. 1B, 2A and C, 5C, and 6C.

RNA extraction and real-time quantitative PCR. Total RNA was extracted from cells with the RNeasy minikit (Qiagen) and subjected to cDNA synthesis with random hexamer primers and Moloney murine leukemia virus (M-MLV) reverse transcriptase (Invitrogen) according to the manufacturer's instructions. Real-time quantitative PCR was performed with FastStart Universal SYBR (Roche) and ABI Prism 7900 (Life Technologies). The PCR primers employed in the present study are listed in Table S4 in the supplemental material.

Immunoprecipitation and immunoblot analysis. COS7 cells were treated with the proteasome inhibitor MG132 (Peptide Institute) at a concentration of 10 μM for 4 h and subjected to preparation as whole-cell extracts with lysis buffer (50 mM Tris-HCl [pH 8.0], 10% glycerol, 100 mM NaF, 50 mM NaCl, 2 mM EDTA, 2 mM sodium orthovanadate, 10 mM sodium pyrophosphate, 10 mM β-glycerophosphate, 0.1% NP-40, 1 mM phenylmethylsulfonyl fluoride (PMSF), and 1× protease inhibitor cocktail [Roche]). The whole-cell extracts were subjected to immunoprecipitation with anti-Flag M2 affinity gels (Sigma) at 4°C for 2 h. After the anti-Flag M2 affinity gels were washed with wash buffer (50 mM Tris-HCl [pH 7.4], 150 mM NaCl, and 0.1% NP-40) three times, the immunocomplexes were eluted by boiling in SDS sample buffer and subjected to immunoblot analysis using the antibodies indicated in the figures. The blots were treated with a horseradish peroxidase-conjugated secondary antibody (Invitrogen) and were developed with an enhanced chemiluminescence (ECL) kit (GE Healthcare).

Chromatin immunoprecipitation. HeLa cells grown in a 100-mm dish were cross-linked in 1% formaldehyde for 10 min, followed by quenching with 1/10 volume of 1.25 M glycine solution and two washes with phosphate-buffered saline (PBS). The cells were lysed in cell lysis buffer (5 mM Tris-HCl [pH 8.0], 85 mM KCl, 0.5% NP-40, 1 mM PMSF, and 1× protease inhibitor cocktail). Nuclear extracts were prepared by treating the nuclear pellets with ChIP SDS lysis buffer (50 mM Tris-HCl [pH 8.0], 10 mM EDTA, 1% SDS, 1 mM PMSF, and 1× protease inhibitor cocktail), followed by sonication using a Bioruptor (Tosho Electric Co., Ltd.). Proteins were immunoprecipitated in ChIP dilution buffer (16.7 mM Tris-HCl [pH 8.0], 167 mM NaCl, 1.2 mM EDTA, 0.01% SDS, 1.1% Triton X-100, 1 mM PMSF, and 1× protease inhibitor cocktail) using the antibodies indicated in the figures and Dynabeads protein G (Invitrogen). The beads were washed with low-salt wash buffer (20 mM Tris-HCl [pH 8.0], 150 mM NaCl, 2 mM EDTA, 0.1% SDS, and 1% Triton X-100), high-salt wash buffer (20 mM Tris-HCl [pH 8.0], 500 mM NaCl, 2 mM EDTA, 0.1% SDS, and 1% Triton X-100), lithium wash buffer (10 mM Tris-HCl [pH 8.0], 250 mM LiCl, 1% deoxycholate, 1 mM EDTA, and 1% NP-40), and Tris-EDTA (TE) buffer. Cross-linking was reversed overnight at 65°C in ChIP elution buffer (1% SDS and 50 mM $NaHCO_3$). ChIPed DNA was then treated with RNase A and proteinase K, purified with a QIAquick PCR purification kit (Qiagen), and analyzed by real-time quantitative PCR.

Bioluminescence recordings. HeLa cells were transfected with a Ub-FL reporter in combination with the indicated siRNAs or 3× Flag Nrf1 (wild-type or S497A mutant) vectors using Lipofectamine 2000. Forty-eight hours after transfection, the cells were treated with 0.1 mM D-luciferin (Toyobo), and bioluminescence was measured and integrated for 1 min at 10-min intervals with a luminometer (AB-2550 Kronos Dio; Atto). Epoxomicin was added to the culture medium 1 to 2 h after the start of the measurement.

Luciferase reporter assay. Cells expressing the reporters indicated in the legends for Fig. 3A and B, 5A and D to F, and 6 were lysed, and the luciferase activities were measured with the PicaGene luciferase assay system (Toyo Ink) and a Berthold Lumat LB9507 luminometer.

Measurement of proteasome activity. HeLa cells transfected with the siRNAs indicated in the figures were treated with 10 nM epoxomicin for 24 h. The proteasome activity was determined by measuring chymotrypsin activity with Proteasome-Glo chymotrypsin-like cell-based assay (Promega) according to the manufacturer's instructions.

FIG 1 Nrf1 regulates the expression of proteasome subunit genes that are induced by proteasome inhibition in HeLa cells. (A) siRNA-mediated knockdown of Nrf1. HeLa cells transfected with control (Ctrl) siRNA or Nrf1 siRNA were treated with DMSO or 1 μM MG132 for 16 h. mRNA expression levels of Nrf1 were determined by real-time quantitative PCR analysis. The values were normalized to 18S rRNA values and presented as the means plus standard deviations (SD) (error bars) ($n = 3$). (B) MG132 induces the accumulation of Nrf1 proteins. HeLa cell extracts were prepared at the indicated time points after 1 μM MG132 treatment and subjected to immunoblot analysis with anti-Nrf1 (αNrf1) (H-285) antibody. αα-tubulin, anti-α-tubulin antibody. (C) Nrf1-dependent induction of proteasome genes. The mRNA expression levels of the indicated genes were determined by real-time quantitative PCR. The expression level in the cells transfected with the control siRNA and treated with DMSO was set at 1. The values were normalized to 18S rRNA values and presented as the means plus SD ($n = 3$). (D) The heat map shows the mRNA expression levels of the indicated genes that correspond to the graphs in Fig. 1C and data not shown. The values were normalized to 18S rRNA values and presented as the means of at least three replicates. The N/C ratio is the ratio of the expression level in Nrf1 siRNA-treated cells to the expression level in control siRNA-treated cells with MG132 treatment. The color bar indicates the range of the expression ratios in log space. (E) Time course of expression of PSMC4, PSMA4, GSTA4, and NQO1 upon MG132 treatment. The values were normalized to 18S rRNA values and presented as the means ± SD ($n = 5$).